Medical Physics
The International Journal of Medical Physics Research and Practice

Comparative dose evaluations between XVI and OBI cone beam CT systems using Gafchromic XRQA2 film and nanoDot optical stimulated luminescence dosimeters

Tawfik Giaddui, Yunfeng Cui, James Galvin, Yan Yu, and Ying Xiao

Citation: Medical Physics **40**, 062102 (2013); doi: 10.1118/1.4803466
View online: http://dx.doi.org/10.1118/1.4803466
View Table of Contents: http://scitation.aip.org/content/aapm/journal/medphys/40/6?ver=pdfcov
Published by the American Association of Physicists in Medicine

Comparative dose evaluations between XVI and OBI cone beam CT systems using Gafchromic XRQA2 film and nanoDot optical stimulated luminescence dosimeters

Tawfik Giaddui, Yunfeng Cui, James Galvin, Yan Yu, and Ying Xiao[a)]
Department of Radiation Oncology, Thomas Jefferson University, Philadelphia, Pennsylvania 19107

(Received 7 January 2013; revised 24 March 2013; accepted for publication 12 April 2013; published 13 May 2013)

Purpose: To investigate the effect of energy (kVp) and filters (no filter, half Bowtie, and full Bowtie) on the dose response curves of the Gafchromic XRQA2 film and nanoDot optical stimulated luminescence dosimeters (OSLDs) in CBCT dose fields. To measure surface and internal doses received during x-ray volume imager (XVI) (Version R4.5) and on board imager (OBI) (Version 1.5) CBCT imaging protocols using these two types of dosimeters.
Methods: Gafchromic XRQA2 film and nanoDot OSLD dose response curves were generated at different kV imaging settings used by XVI (software version R4.5) and OBI (software version 1.5) CBCT systems. The settings for the XVI system were: 100 kVp/F0 (no filter), 120 kVp/F0, and 120 kVp/F1 (Bowtie filter), and for the OBI system were: 100 kVp/full fan, 125 kVp/full fan, and 125 kVp/half fan. XRQA2 film was calibrated in air to air kerma levels between 0 and 11 cGy and scanned using reflection scanning mode with the Epson Expression 10000 XL flat-bed document scanner. NanoDot OSLDs were calibrated on phantom to surface dose levels between 0 and 14 cGy and read using the inLight^{TM} MicroStar reader. Both dosimeters were used to measure in field surface and internal doses in a male Alderson Rando Phantom.
Results: Dose response curves of XRQA2 film and nanoDot OSLDs at different XVI and OBI CBCT settings were reported. For XVI system, the surface dose ranged between 0.02 cGy in head region during fast head and neck scan and 4.99 cGy in the chest region during symmetry scan. On the other hand, the internal dose ranged between 0.02 cGy in the head region during fast head and neck scan and 3.17 cGy in the chest region during chest M20 scan. The average (internal and external) dose ranged between 0.05 cGy in the head region during fast head and neck scan and 2.41 cGy in the chest region during chest M20 scan. For OBI system, the surface dose ranged between 0.19 cGy in head region during head scan and 4.55 cGy in the pelvis region during spot light scan. However, the internal dose ranged between 0.47 cGy in the head region during head scan and 5.55 cGy in the pelvis region during spot light scan. The average (internal and external) dose ranged between 0.45 cGy in the head region during head scan and 3.59 cGy in the pelvis region during spot light scan. Both Gafchromic XRQA2 film and nanoDot OSLDs gave close estimation of dose (within uncertainties) in many cases. Though, discrepancies of up to 20%–30% were observed in some cases.
Conclusions: Dose response curves of Gafchromic XRQA2 film and nanoDot OSLDs indicated that the dose responses of these two dosimeters were different even at the same photon energy when different filters were used. Uncertainty levels of both dosimetry systems were below 6% at doses above 1 cGy. Both dosimetry systems gave almost similar estimation of doses (within uncertainties) in many cases, with exceptions of some cases when the discrepancy was around 20%–30%. New versions of the CBCT systems (investigated in this study) resulted in lower imaging doses compared with doses reported on earlier versions in previous studies. [http://dx.doi.org/10.1118/1.4803466]

Key words: CBCT, XVI/OBI, Gafchromic film, nanoDot OSLD, image dose

I. INTRODUCTION

Image-guided radiotherapy (IGRT) is an emerging radiation treatment modality,[1] involves locating the target position by using imaging modalities in direct conjunction with the treatment. It is commonly performed using kV cone beam computed tomography (CBCT).[1–4] In CBCT, an x-ray source and a flat panel detector are mounted to the gantry of the linear accelerator to acquire planar images, and also to acquire multiple projections of the patients during a 200° or 360° rotation resulting in a cone-beam CT scan to provide a three-dimensional (3D) volumetric knowledge about the patient's anatomy for each fraction.[1–3] It is possible with these images to locate the target volume directly before a treatment session and to reposition the patient based on matching of CBCT and treatment planning CT. CBCT however results in an additional dose to the patient, especially to healthy tissues and organs as the imaged volume is larger than the

treated volume, and its use needs to be justified by the clinical needs. Therefore, dose measurements for different imaging protocols are of utmost interest, especially when daily imaging is intended.[1–4] Many studies have been conducted to estimate image doses, acquired during various imaging protocols of different versions of different CBCT systems, in patients and in phantoms using different dosimeters.[3–19]

Gafchromic XRQA2 film and nanoDot optical stimulated luminescence dosimeters (OSLDs) are relatively new dosimeters, which are used for the patient-specific *in vivo* dosimetry. However, these two dosimeters were shown to be energy dependent in the kV energy range.[20–24] CBCT can be performed for different kVps, ranging from approximately 80 to 140 in addition to the fact that different types of filters (e.g., half Bowtie and full Bowtie) are in use and these filters are expected to slightly change the beam spectra and eventually dose response curves of the dosimeters. Most of the previous studies on the energy dependence of nanoDot OSLD focused only on the response of the dosimeter at different beam energies and were not performed in CBCT fields. For the Gafchromic film, however, a previous study[3] reported on the dose response curves for the XRQA film (an older model of the Gafchromic film, which is replaced by the XRQA2 model used in this study) at different beam qualities of the on board imager (OBI) CBCT system [100 kVp full fan (FF), 125 kVp half fan (HF) and FF)]. We also showed, in our previous study,[20] dose response curves of the XRQA2 film at two different beam qualities of the x-ray volume imager (XVI) CBCT system [100 kVp/F1 and 120 kVp/F1 (Bowtie filter)], nevertheless, this study did not evaluate the effect of different filters used by the XVI CBCT system. Both Varian and Elekta released the latest versions of their CBCT imaging protocols, namely, the OBI version 1.5 and the XVI version R4.5, respectively. These two versions are in use in clinics and it is appropriate to report on the imaging dose imparted using their different protocols. The aims of the present work are: evaluating the effects of beam energy (kVp) and filters on the dose response curves of the Gafchromic XRQA2 film and nanoDot OSLD to ensure accurate estimation of image doses and measuring the surface and internal imaging dose acquired during different XVI (software version R4.5) and OBI (software version 1.5) CBCT systems imaging protocols.

II. MATERIALS AND METHODS

II.A. Cone beam systems

CBCT systems evaluated in this study are the XVI (software version R4.5) mounted on the Elekta Synergy (Elekta, Crawley, UK) linac and the OBI (software version 1.5) mounted on the Varian True Beam (Varian Medical systems, Palo Alto, CA) linac. Detailed description of the operation of these systems can be found in Refs. 3, 7, 9, and 17. Tables I and II list a complete description of the machines settings used for the different protocols investigated in this study for the XVI and the OBI systems, respectively.

II.B. Dosimetry systems

II.B.1. Gafchromic XRQA2 film dosimetry system

Our film dosimetry system consists of Gafchromic XRQA2 (International Specialty Products, Wayne, NJ) films, a Farmer-type ion chamber calibrated for absolute dosimetry [at the University of Wisconsin Accredited Dosimetry Laboratory (UW-ADCL)] and an Epson Expression 10000 XL flat-bed document scanner (Seiko Epson Corporation, Nagano, Japan). Gafchromic XRQA2 film is designed specifically as a QA tool for radiology and dosimetry applications.[25] It is sensitive to dose range 0.1–20 cGy and energy range 20–200 kVp.[25] This film model is a reflective-type film consisting of five layers: 97 μm thick yellow polyester layer, 15 μm thick pressure sensitive adhesive layer, 25 μm thick active layer, 3 μm thick surface layer, and 97 μm thick opaque white polyester layer. The active layer of the film nominally consists of H, C, N, O, Li, Br, and Cs. The inclusion of white opaque polyester film layer necessitated film digitization with a reflective densitometer.[3,26,27] However, we proved in our previous study on the characteristics of this film model,[20] that this type of films can also be analyzed using transmission densitometer.

II.B.2. Optical stimulated luminescence dosimetry system

The OSLD system is inLight™ OSL system (Landauer, Inc., Glenwood, IL).[21] It consisted of nanoDot dosimeters, MicroStar reader, and an external PC with dosimetry software. The nanoDot dosimeters made of OSL active element

TABLE I. Different kV CBCT imaging protocols in Elekta (XVI R4.5) and their important parameters.

Protocols	Collimator/ filter	Tube voltage (kVp)	Total mAs	Frames	Scan angle	kV x-ray source start/stop angle
Head and neck	S20/F0	100	36.6	366	200	320°–160°
Fast head and neck	S20/F0	100	18.3	183	200	320°–160°
Chest M20	M20/F1	120	1056.0	660	360	…
Left chest half	S20/F0	100	264.0	660	200	70°–269°
Symmetry	S20/F0	120	422.4	1320	200	270°–110°
Pelvis M20	M20/F1	120	1056.0	660	360	…
Prostate seed S10	S10/F0	120	117.1	366	200	320°–160°

TABLE II. Different kV CBCT imaging protocols in Varian True Beam (OBI 1.5) and their important parameters.

Protocol	Fan type	Tube voltage (kVp)	Total mAs	Frames	Trajectory
Head	Full fan	100	264	367	Full
Thorax	Half fan	125	264	660	Full
Thorax slow	Half fan	125	252	630	Full
Thorax very slow	Half fan	125	336	840	Full
Pelvis	Half fan	125	1056	660	Full
Spot light	Full fan	125	1320	367	Full

(Al_2O_3:C), 5 mm in diameter, 0.1 mm thick, placed in a 10 × 10 × 2 mm light proof plastic housing.[24] The housing opens automatically during the reading process. They can be used to measure doses in the range from 0.01 to 1500 cGy in the energy range 5 keV up to 20 MeV and have linear response up to 300 cGy.[21] The nanoDot OSL have received great attention and many studies were conducted to investigate their properties at the MV (Refs. 22 and 28) and kV (Refs. 22 and 29) energy levels. The MicroStar reader uses a green light emitting diode (LED) array, with the wavelength centered at 530 nm. The operation mode of the reader is called the continuous wave simulation mode and the reading time is approximately 1 s.[28] The MicroStar reader is provided with different calibration curves to account for the kV and MV energy ranges. The reader removes only a small portion of the signal (about 0.05%) each time the dosimeter is read.[23] Hence, a dosimeter can easily be reread if there is any doubt about the validity of a particular reading.

II.C. Half value layer (HVL) measurements

CBCT can be performed for different kVps, also the beam energy may change slightly due to use of filters (Bowtie filter). Hence, it is important to measure the first HVL of each beam, as HVL values are needed to determine the absorbed dose to water at the phantom surface according to the AAPM TG61 protocol.[30] Half value layers for all CBCT setting used in this study were measured using a 0.6 CC Farmer ionization chamber (calibrated for absolute dosimetry at the UW-ADCL) and aluminum attenuators of different thicknesses. The chamber was placed at 100 cm from the beam and the attenuators at 50 cm. Beams were collimated using homemade collimator and the attenuator thicknesses were increased successively. The half value layers for the XVI CBCT 100 kVp/F0, 120 kVp/F0, and 120 kVp/F1 beams were 5.61, 6.14, and 6.45 mm Al, respectively. The half value layers for the kV OBI CBCT 100 and 125 kVp/FF beams were 6.93 and 7.72 mm Al, respectively.

II.D. Calibration of dosimeters

II.D.1. Calibration of Gafchromic XRQA2 film

We reported in our previous paper[20] that the Gafchromic XRQA2 film exhibits energy dependence in the kV energy ranges. However, the use of different types of filters in CBCT fields CBCT might affect the dose response curves of the film and eventually the accuracy of the measured doses. Hence, it is important to generate a dose response curve for each CBCT setting. To generate calibration curves, film pieces 2 × 3 cm (lot #A04280904A) were irradiated in air at the source to film distance of 75 cm using 100 kVp/F0 (no filter), 120 kVp F0 and F1 (Bowtie filter) photon beams of the kV XVI cone beam CT system and 100 kVp full fan (full Bowtie), 125 kVp half (half bowtie), and full fan photon beams of the kV OBI cone beam CT system. Eleven dose points ranging from 0 to 11 cGy were used to generate each calibration curve. Films were scanned using the reflection mode of the Epson Expression 10000 XL flat-bed document scanner. Details of the calibration and the scanning processes of the Gafchromic XRQA2 film can be found in our previous study on this film model.[20] Experimental and fitting uncertainties for each dose point of each calibration curve in addition to total uncertainty were calculated using the procedure described by Tomic *et al.*[3]

II.D.2. Calibration of nanoDot optical stimulated luminescence dosimeters

The response of the Al_2O_3:C exhibits significant energy dependence at energies typically used for diagnostic radiology.[21–24] The Vendor provides a calibration curve for the kV energy level, which is generated using reference dosimeters that are calibrated on polymethyl-methacrylate (PMMA) material at 80 kVp.[24] Correction factors can also be used with the calibration curve to account for the energy dependence.[24] To generate a calibration curve for the nanoDot OSLDs, the dosimeters were irradiated on 5 cm thick PMMA slab using 120 kVp F0/F1 photon beams for the XVI system, 100 kVp full fan, and 125 kVp half fan and full fan photon beams for the OBI system. For each calibration curve, 6–10 dose points ranging from 0 to 12 cGy were used. Three nanoDot dosimeters were used for each calibration point. Dose points were correlated to absolute air kerma levels measured free in air using the 0.6 cc Farmer ionization chamber and converted to dose in water at the phantom surface according to AAPM TG61.[30] Each dosimeter was read three times using the MicroStar reader, thus nine readings were used for each calibration point. The calibration curve represents the relation between average reading of the photomultiplier tube (PMT) of the MicroStar reader and dose. The MicroStar reader software calculates the calibration factor, which converts the PMT reading to dose. Uncertainty levels were calculated as mentioned in Sec. II.D.1.

II.E. Surface dose measurements

Surface dose measurements for all CBCT imaging protocols listed in Tables I and II were measured on the surface of a male Alderson Rando Phantom (Alderson Research Laboratories, Inc., Long Island City, NY). The surface doses were measured in three body regions (head and neck, thorax, and pelvis) at four different places (anterior, posterior, right lateral, and left lateral) in the irradiated area using Gafchromic

XRQA2 film and nanoDot OSLDs. The phantom was placed at isocenter. Two Gafchromic film pieces (2 × 3 cm each) and two nanoDot OSLDs were taped on the surface of the phantom at each measurement location. Thus, eight film pieces and eight OSLDs were used for measuring the surface dose acquired during the acquisition of each imaging protocol. XVI surface dose was measured using two different shots (one for the film and one for the OSLD) while OBI surface dose was measured using single shot. Film response was converted to surface dose using the appropriate calibration curve as described by Tomic *et al.*[3] The OSLDs were read using the MicroStar reader using the appropriate calibration curve, each dosimeter was read three times and the average reading was calculated. The dose at each location, whether it was measured by the film or the OSLD, represents the average dose as measured by the two dosimeters of each type.

II.F. Near surface and central dose measurements

Gafchromic film pieces (2 × 3 cm) and nanoDot OSLDs were also placed between pieces of the male Alderson Rando Phantom to measure near surface and central doses. Here, one film piece and two OSLDs were placed at a distance of around 1.5 cm from the surface of the phantom at each of the four places (anterior, posterior, right lateral, and left lateral), in addition to that, one film piece and two OSLDs were placed at the center of the phantom in the irradiation region. All dosimeters were sandwiched between two slabs of the phantom and a sheet of bolus was placed between the two slabs to prevent any air gap. Figure 1 shows a schematic diagram of the position of the film relative to nanoDot OSLD in internal dose measurements.

III. RESULTS

III.A. Calibration of Gafchromic XRQA2 film for kV XVI/OBI CBCT image dose

Figure 2 shows the dose response curves of the film for the kV XVI CBCT (100 kVp/F0, 120 kVp/F0, and 120 kVp/F1) irradiation settings. Here, the air kerma values were plotted versus the net reflectance change of the film. The dose response curves were fitted using the same fitting function reported in our previous study.[20] The 120 kVp dose response curves of the film generated with F1 (Bowtie) and F0 (no filter) filters were found to differ by 5%–7% when the air kerma changed between 2 and 5 cGy. This was in fact less than the observed difference (more than 15%, especially at low air kerma) in the dose response curves when different energies (100 and 120 kVp) and same filter (F1) were used. Figure 3 shows the dose response curves of the film for the kV OBI CBCT (100 kVp/FF, 125 kVp/HF, and 125 kVp/FF) irradiation settings. As can be seen, the dose response curves of the 100 and 125 kVp/FF beams differed by about 10%–17% when the air kerma changed between 0.5 and 9 cGy. The dose response curves of the 125 kVp/FF and 125 kVp/HF photon beams of the OBI CBCT system were very close to each other (almost overlapped), the variations in the response curves of these two settings varied between −4% and 3%.

Figures 4(a) and 4(b) show the variation of the percentage relative uncertainties (the percentage of the quotient of the total uncertainty and the air kerma) with air kerma values for the XVI 120 kVp/F1 and the OBI 125 kVp/HF irradiation settings, respectively, as examples of uncertainty analysis for film dose response curves. For all XVI and OBI irradiation settings, the uncertainty was high at low air kerma values and decreased with increased air kerma values. The uncertainty reached 18% at about 0.2 cGy for the XVI 120 kVp/F1

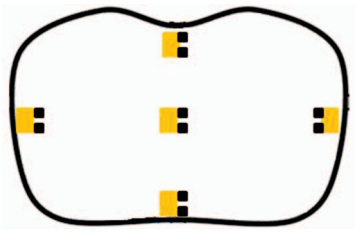

FIG. 1. A schematic diagram shows the position of film relative to nanoDot OSLD in internal dose measurements. Rectangles represent XRQA2 film, small squares represent nanoDot OSLD.

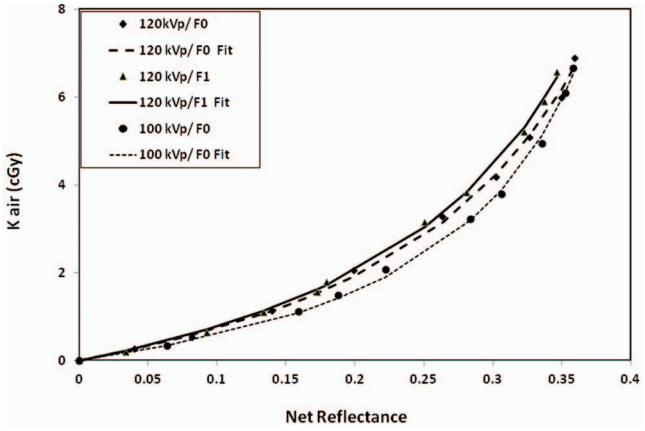

FIG. 2. Dose response curves of the film for the kV XVI CBCT (100 kVp/F0; 120 kVp/F0, and 120 kVp/F1) irradiation settings.

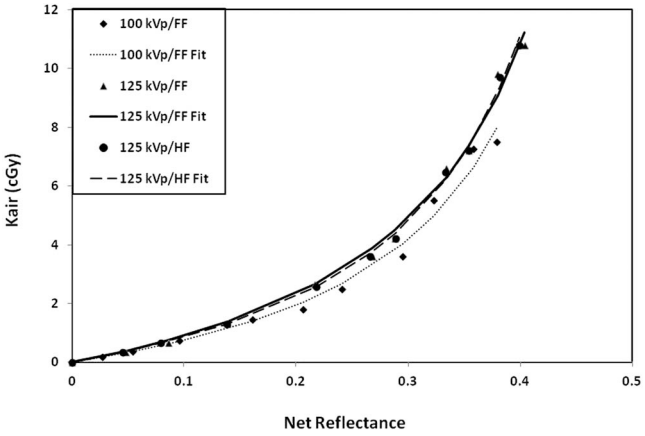

FIG. 3. Dose response curves of the film for the kV OBI CBCT (100 kVp/FF, 125 kVp/HF, and 125 kVp/FF) irradiation settings.

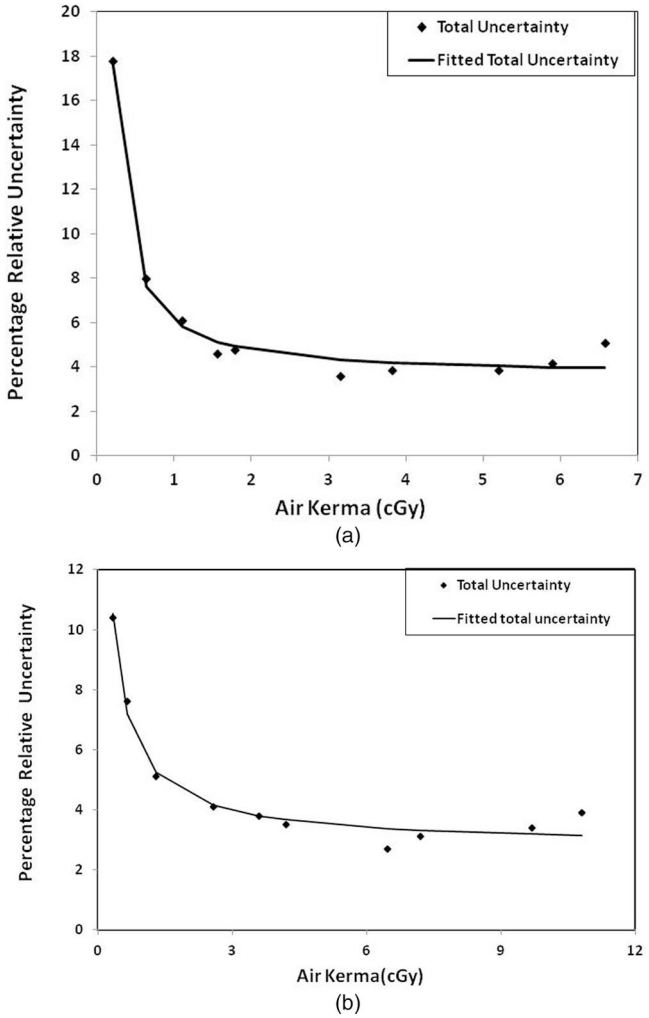

FIG. 4. Variation of the percentage relative uncertainty with air kerma. (a) For the XVI 120 kVp/F1 irradiation setting. (b) For the OBI 125 kVp/HF irradiation setting.

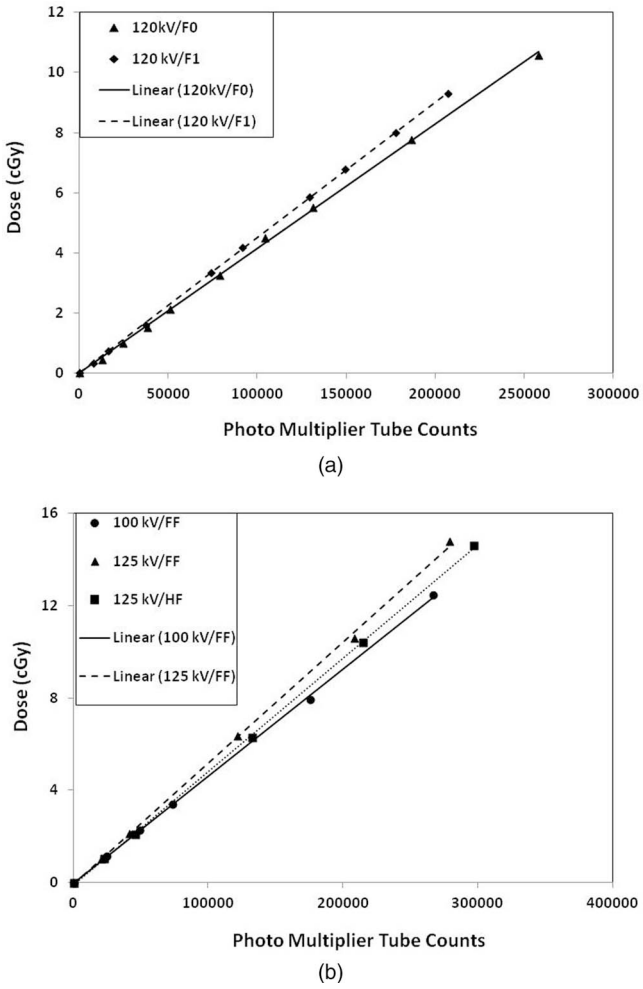

FIG. 5. Dose response curves of the nanoDot OSLDs. (a) For kV XVI CBCT (120 kVp/F0 and 120 kVp/F1) irradiation setting. (b) For kV OBI CBCT (100 kVp/FF, 125 kVp/HF, and 125 kVp/FF) irradiation settings.

curve and ranged from 3% to 6% (for both CBCT systems) at air kerma values above 1 cGy. The percentage relative uncertainty curves were used to calculate the uncertainty associated with each kV XVI or kV OBI point dose measured using the Gafchromic XRQA2 film.

III.B. Calibration of nanoDot optical stimulated luminescence dosimeters for kV XVI/OBI CBCT image dose

Figure 5(a) shows the dose response curves of the nanoDot OSLDs for kV XVI CBCT (120 kVp/F0 and 120 kVp/F1) irradiation settings. Here, the surface dose was plotted versus the average reading of the photomultiplier tube of the MicroStar reader. As can be seen, the dose response curves were linear and differed by about 8%–9% at almost all dose points. Figure 5(b) shows the dose response curves of the nanoDot OSLDs for the three kV CBCT OBI system (100 kVp/FF, 125 kVp/HF, and 125 kVp/FF) irradiation settings. The dose response curves were again linear. The difference in the response curves of the 100 and 125 kVp/FF was about 10%–11%. There was also a difference between the dose response curves of the 125 kVp/HF and 125 kVp/FF, the variation was between 7% and 8%. Figures 6(a) and 6(b) show the percentage relative uncertainty versus dose for the kV XVI 120 kVp/F1 and the kV OBI 100 kV/FF irradiation settings, respectively. The percentage relative uncertainty was as high as 12% at doses of about 0.44 cGy and ranged between 2% and 5% at doses above 1 cGy. The percentage relative uncertainty curves were used to calculate the uncertainty associated with each kV XVI or kV OBI point dose measured using the nanoDot OSLDs.

III.C. kV XVI CBCT dose measurements using Gafchromic XRQA2 film and nanoDot OSLDs

Table III lists the surface dose at four locations (anterior, posterior, right lateral, and left lateral) on the phantom surface acquired during different kV XVI CBCT imaging protocols. The surface dose measured by the XRQA2 film ranged between 0.02 and 4.99 cGy. The lowest surface dose was observed in the head and neck region (posterior) when the fast head and neck protocol was used, while the highest surface

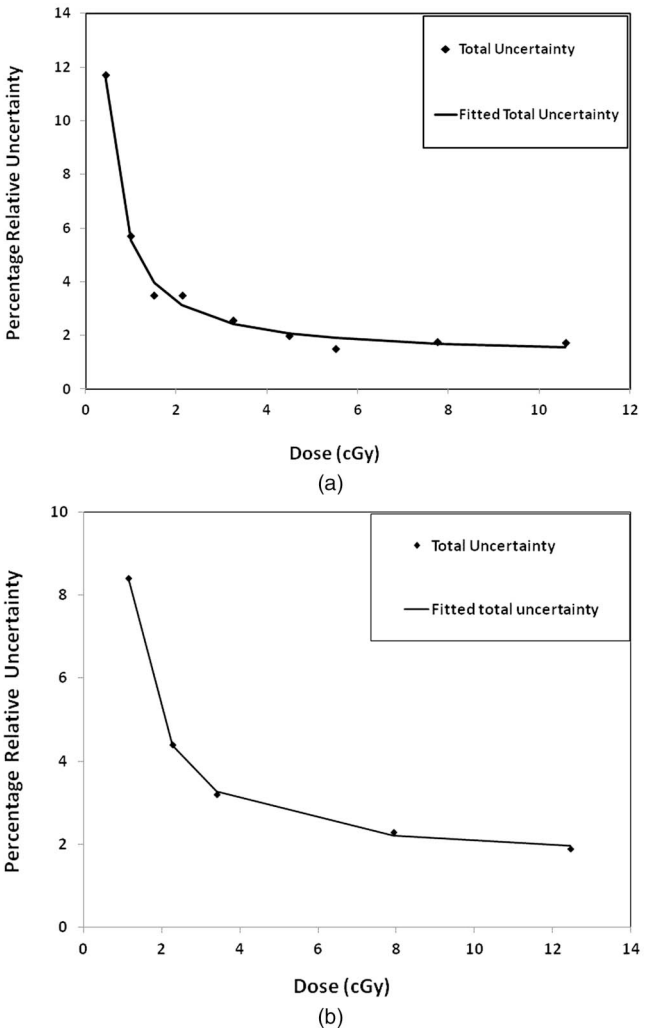

FIG. 6. Variation of the percentage relative uncertainty with dose. (a) for the XVI CBCT 120kVp/F1 irradiation setting. (b) For the OBI CBCT 100 kVp/FF irradiation setting.

dose was noticed in the chest region (anterior) when the symmetry protocol was used. The surface dose measured by the nanoDot OSLDs ranged between 0.04 and 4.53 cGy. Here, the lowest dose was also observed in the head and neck region (right lateral) during the fast head and neck scan and the highest dose was again observed in the chest region (anterior) during the symmetry scan. Low dose values, as those reported for fast head and neck protocol (measured using film and OSLD), were associated with very high uncertainties, as uncertainties increased sharply at very low dose values.

Table IV lists the internal dose acquired using the same imaging protocols at five different locations inside the phantom (near anterior surface, near posterior surface, near right lateral surface, near left lateral surface, and phantom center). The internal dose measured by both dosimetry systems indicated that the lowest dose was observed when fast head and neck protocol was used (0.03 cGy measured by the film and 0.02 cGy measured by the OSLD) and the highest dose was noticed when the chest M20 protocol was used (2.7 cGy by film and 3.17 cGy by the OSLD).

Different point doses were associated with different uncertainties and some of these uncertainties were very high (at very low doses), in addition to that, point doses for each imaging protocol were measured at nine different locations. Hence, it was decided to calculate the weighted average dose (The weighted average dose is the average dose calculated using the different nine points doses with consideration given to the uncertainty associated with each point dose. Here, weights were calculated to all point doses based on their uncertainties as it was shown in Tomic *et al.*[3] The weighted average dose will be referred to as average dose in the remainder of the text.) acquired during each imaging protocol as measured by XRQA2 film and nanoDot OSLDs in order to make direct comparison between the results obtained using both dosimetry systems and compare them with the nominal dose given by the Vendor. Table V lists the average dose as measured by the XRQA2 film and nanoDot OSLDs and the nominal dose (measured by the Vendor) for all kV XVI CBCT imaging protocols investigated in this study.

III.D. kV CBCT True Beam (OBI 1.5) dose measurements using Gafchromic XRQA2 film and nanoDot OSLDs

Table VI lists the surface dose at four locations (anterior, posterior, right lateral, and left lateral) on the phantom surface acquired during six imaging protocols using the kV CBCT in Varian True Beam (OBI 1.5) scans. The surface dose measured by the XRQA2 film ranged between 0.19 and 4.19 cGy, the lowest dose was noticed in the head and neck region (ante-

TABLE III. Surface dose (cGy) acquired during different XVI CBCT imaging protocols as measured by Gafchromic XRQA2 film and nanoDot OSLDs.

	Anterior		Posterior		Right lateral		Left lateral	
Imaging protocol	nanoDot	XRQA2	nanoDot	XRQA2	nanoDot	XRQA2	nanoDot	XRQA2
Head and neck	0.15 ± 0.05	0.14 ± 0.04	0.11 ± 0.05	0.09 ± 0.04	0.08 ± 0.06	0.09 ± 0.04	0.21 ± 0.05	0.19 ± 0.04
Fast head and neck	0.08 ± 0.06	0.07 ± 0.04	0.07 ± 0.06	0.02 ± 0.04	0.04 ± 0.06	0.03 ± 0.04	0.10 ± 0.05	0.10 ± 0.04
Chest M20	2.67 ± 0.07	3.39 ± 0.15	2.19 ± 0.07	3.06 ± 0.13	2.18 ± 0.07	3.01 ± 0.13	1.92 ± 0.06	2.79 ± 0.12
Left chest half	0.23 ± 0.05	0.25 ± 0.04	0.86 ± 0.05	0.87 ± 0.06	0.37 ± 0.05	0.34 ± 0.04	0.60 ± 0.05	0.65 ± 0.05
Symmetry	4.53 ± 0.09	4.99 ± 0.21	0.63 ± 0.05	0.64 ± 0.05	1.92 ± 0.06	2.13 ± 0.10	2.62 ± 0.07	3.20 ± 0.14
Pelvis M20	2.84 ± 0.07	3.70 ± 0.16	2.44 ± 0.07	3.15 ± 0.14	2.19 ± 0.07	2.58 ± 0.12	1.87 ± 0.06	2.51 ± 0.11
Prostate seed S10	0.85 ± 0.05	1.01 ± 0.06	0.44 ± 0.05	0.44 ± 0.04	0.16 ± 0.05	0.12 ± 0.04	0.78 ± 0.05	0.96 ± 0.06

TABLE IV. Internal dose (cGy) acquired during different XVI CBCT imaging protocols as measured by Gafchromic XRQA2 film and nanoDot OSLDs.

	Near anterior surface		Near posterior surface		Near right lateral surface		Near left lateral surface		Central dose	
Protocol	nanoDot	XRQA2	nanoDot	XRQA2	nanoDot	XRQA2	nanoDot	XRQA2	nanoDot	XRQA2
Head and neck	0.11 ± 0.05	0.06 ± 0.04	0.04 ± 0.06	0.07 ± 0.04	0.04 ± 0.06	0.04 ± 0.04	0.13 ± 0.05	0.11 ± 0.04	0.07 ± 0.06	0.06 ± 0.04
Fast head and neck	0.06 ± 0.06	0.04 ± 0.04	0.06 ± 0.06	0.03 ± 0.04	0.03 ± 0.06	0.03 ± 0.04	0.08 ± 0.05	0.05 ± 0.04	0.02 ± 0.06	0.03 ± 0.04
Chest M20	3.17 ± 0.08	2.70 ± 0.12	2.21 ± 0.07	1.80 ± 0.09	2.63 ± 0.07	2.13 ± 0.10	2.31 ± 0.07	1.90 ± 0.09	2.75 ± 0.07	2.68 ± 0.12
Symmetry	2.7 ± 0.07	2.37 ± 0.11	0.46 ± 0.05	0.51 ± 0.05	1.32 ± 0.06	1.24 ± 0.07	2.08 ± 0.07	1.98 ± 0.09	1.05 ± 0.06	1.35 ± 0.07
Pelvis M20	2.61 ± 0.07	2.53 ± 0.11	2.28 ± 0.07	1.88 ± 0.09	2.14 ± 0.07	1.79 ± 0.09	2.03 ± 0.07	1.75 ± 0.09	2.1 ± 0.07	1.8 ± 0.09
Prostate seed S10	0.53 ± 0.05	0.53 ± 0.05	0.27 ± 0.05	0.26 ± 0.04	0.08 ± 0.05	0.16 ± 0.04	0.69 ± 0.05	0.68 ± 0.05	0.23 ± 0.05	0.27 ± 0.04

rior) when the head protocol was used, while the highest surface dose was observed in the pelvis region (anterior) when the spot light protocol was used. The surface dose measured by the nanoDot OSLDs ranged between 0.27 and 4.55 cGy, the lowest and the highest surface doses measured by the OSLDs were observed in the same locations and for the same imaging protocols as those measured by the film. Although, the estimation of both XRQA2 film and the nanoDot OSLDS to the lowest and highest doses looked different, they were in fact close to each other when the uncertainties associated to these point doses were taken into consideration.

Table VII lists the internal dose acquired using the same imaging protocols at five locations inside the phantom (near anterior surface, near posterior surface, near right lateral surface, near left lateral surface, and phantom center). The internal dose measured by XRQA2 film ranged between 0.47 cGy (near posterior surface when head imaging protocol was used) and 5.48 cGy (near anterior surface when the spot light imaging protocol was acquired). The internal dose measured by the nanoDot OSLDs ranged between 0.51 cGy (near left lateral surface when thorax imaging protocol was acquired) and 5.55 cGy (near anterior surface when spot light imaging protocol was acquired). The highest internal dose estimated by both dosimetry systems were observed in the same location and for the same imaging protocol. Table VIII lists the average doses as measured by XRQA2 film and nanoDot OSLDs and the weighted cone beam CT dose index (provided by the Vendor) for all kV OBI CBCT imaging protocols investigated in this study.

TABLE V. Average dose (cGy) as measured by XRQA2 film and nanoDot OSLDs and nominal doses (cGy) for kV XVI CBCT imaging protocols.

Imaging protocol	nanoDot	XRQA2	Nominal dose[a]
Head and neck	0.11 ± 0.02	0.09 ± 0.01	0.12
Fast head and neck	0.06 ± 0.02	0.05 ± 0.01	0.06
Chest M20	2.41 ± 0.02	2.43 ± 0.04	2.2
Symmetry	1.56 ± 0.02	1.21 ± 0.03	1.55
Pelvis M20	2.26 ± 0.02	2.19 ± 0.04	2.2
Prostate seed S 10	0.45 ± 0.02	0.41 ± 0.02	0.38

[a]Nominal dose measured by the Vendor and displayed in the system software.

IV. DISCUSSION

The dose response of the Gafchromic XRQA2 film at 120 kVp/F0 (no filter) XVI and 120 kVp/F1 (Bowtie filter) XVI CBCT indicated that the response curves can be different even at the same beam energies when different filters are used. The Bowtie (F1) filter hardens the spectrum and therefore affects the dose response curve. The dose response curves of the film using the 125 kVp HF and FF OBI CBCT beams were almost identical, suggesting that the spectra of these two beams were very close to each other. The magnitude of the difference in the film dose response curve for photon beams of same energy but using different filters seemed to be less than the difference in the response curves when different energies and same filters are used. The dose response curves of the nanoDot OSLD dosimeter using both CBCT systems were different when different energies and same filters were used and were also different when same energies and different filters were used. The dose response curves for the OSLD were different even for the 125 kVp HF and FF OBI beams, this result was different from that obtained with the Gafchromic film, where almost identical dose response curves were obtained. Al_2O_3:C nanoDot OSLDs are known to have strong energy dependence at low photon energies[21–24] and the observed variation in the dose response curves of the OSLDs at the 125 kVp HF and FF beams suggests that nanoDot OSLD is more sensitive to small differences in spectra, caused by the use of different filters, than Gafchromic XRQA2 film. The result also indicates that the use of correction factors to allow the reading of the MicroStar reader to be converted from one set of reference condition to another based solely on the differences in the response of the OSLDs at different energies is not sufficient to ensure accurate estimation of measured doses. It is important as demonstrated above to generate a dose calibration curve for every energy/filter combination in order to minimize measurements uncertainty. We did not quantitatively evaluate the impact of the x-ray spectrum variation across its profile, especially across the Bowtie filter, on the film and OSLD readings, as it is beyond the scope of this study. However, we believe that such effect was included to some extent in our dose response curves (created specifically for the imaging protocol in use) as three film/OSLD pieces were placed next to each others for every calibration point and the average response of the three pieces was used for

TABLE VI. Surface dose (cGy) acquired during different OBI CBCT imaging protocols as measured by Gafchromic XRQA2 film and nanoDot OSLDs.

	Anterior		Posterior		Right lateral		Left lateral	
Imaging protocol	nanoDot	XRQA2	nanoDot	XRQA2	nanoDot	XRQA2	nanoDot	XRQA2
Head	0.53 ± 0.11	0.47 ± 0.04	0.27 ± 0.13	0.19 ± 0.03	0.49 ± 0.11	0.44 ± 0.04	0.51 ± 0.11	0.47 ± 0.04
Thorax	0.65 ± 0.10	0.59 ± 0 .04	0.24 ± 0.13	0.41 ± 0.04	0.42 ± 0.11	0.55 ± 0.04	0.29 ± 0.12	0.39 ± 0.04
Thorax Slow	...	0.75 ± 0.05	...	0.48 ± 0.04	...	0.61 ± 0.05	...	0.41 ± 0.04
Thorax very slow	1.02 ± 0.10	0.95 ± 0.06	0.65 ± 0.10	0.65 ± 0.05	0.83 ± 0.10	0.94 ± 0.06	0.51 ± 0.11	0.53 ± 0.04
Pelvis	2.36 ± 0.10	2.96 ± 0.12	2.56 ± 0.10	2.44 ± 0.10	1.74 ± 0.10	1.88 ± 0.09	1.66 ± 0.10	1.65 ± 0.08
Spot light	4.55 ± 0.13	4.19 ± 0.15	3.53 ± 0.11	3.74 ± 0.14	2.43 ± 0.10	2.78 ± 0.11	2.7 ± 0.10	2.68 ± 0.11

every calibration point. The results on the uncertainty analysis indicated that both dosimeters have reasonable uncertainty, ranging between 2% and 6% at doses above 1 cGy. However, the uncertainty was higher at lower doses and was very high at very low doses. This suggests that the readings of both dosimeters at doses well below 0.1 cGy should be treated with care, as the uncertainty can be as high as 100% at such doses.

When doses acquired during different imaging protocols are compared, one can observe, as reported previously in the literatures, a direct relationship between the dose and the total mAs used by the particular imaging protocol. For example, the XVI head and neck protocol (total mAs 36.6) resulted in higher doses (∼45% on the average) compared with the XVI fast head and neck protocol (total mAs 18.3); the XVI chest M20 protocol also resulted in a higher surface dose (∼78% higher) compared with the XVI left chest half protocol; the OBI thorax very slow protocol (336 mAs) resulted in higher (∼28%) average dose than the OBI thorax protocol (264 mAs); and the OBI spotlight imaging protocol (1320 mAs) also resulted in higher (∼37%) average dose than the OBI pelvis protocol (1056 mAs).

Doses delivered to different sites of the body can also be different, for example, doses acquired during pelvis region scans (either the OBI pelvis or the spotlight protocol or the XVI pelvis M20) use higher mAs than protocols that image other sites of the body like the head region and this lead to significantly higher doses to these body regions. These variations in mAs and eventually in doses of different protocols used to image different sites are also related the extent of the body region to be scanned to meet the specific clinical objectives and to image quality, a parameter that is beyond the scope of this study, and was addressed in Refs. 13 and 16. One can also notice that protocols which are used to image a particular region in the body can use significantly different mAs, different energies, filters, and different trajectories to achieve a particular clinical objective and this leads to different doses being delivered to that region of the body. For example, the XVI chest M20 protocol (120 kVp/F1 filter), with full trajectory (360°) uses 1056 mAs while the XVI left chest half protocol (100 kVp/F0), with partial trajectory (200°) uses only 264 mAs. Also, the settings used by OBI pelvis (1056 mAs and half fan) are different from those used by the OBI spotlight (1320 mAs and full fan).

The lateral and vertical dose distributions for all XVI imaging protocols with scan angle of 200° investigated in this study are asymmetrical. This asymmetry in the lateral dose distribution can be noticed from the different dose imparted to left and right lateral sides of the phantom. The surface dose for the left lateral side was always higher than the surface dose for the right lateral side, this observation is consistent with the start and stop angle of the x-ray source, which spends more time toward the left lateral side of the phantom and hence delivers higher dose to this side as compared with the right lateral side. The asymmetry in the vertical dose distributions is obvious in the difference between the anterior and posterior doses acquired during the left chest half and the symmetry protocols. For the left chest half, the posterior dose is much higher than the anterior dose, such a difference is consistent with the start/stop (70°–260°) angle of the x-ray source. For the symmetry protocol, the anterior dose is much higher than the posterior dose and again the difference in dose is consistent with the start/stop (270°–110°) angle of the source.

TABLE VII. Internal dose (cGy) acquired during different OBI CBCT imaging protocols as measured by Gafchromic XRQA2 film and nanoDot OSLDs.

	Near anterior surface		Near posterior surface		Near right lateral surface		Near left lateral surface		Phantom center	
Protocol	nanoDot	XRQA2	nanoDot	XRQA2	nanoDot	XRQA2	nanoDot	XRQA2	nanoDot	XRQA2
Head and neck	0.65 ± 0.10	0.53 ± 0.04	0.52 ± 0.11	0.47 ± 0.04	0.72 ± 0.10	0.66 ± 0.05	0.74 ± 0.10	0.61 ± 0.05	0.71 ± 0.10	0.64 ± 0.05
Thorax	0.77 ± 0.10	0.98 ± 0.06	0.52 ± 0.11	0.56 ± 0.04	0.63 ± 0.10	0.84 ± 0.05	0.51 ± 0.11	0.54 ± 0.04	0.79 ± 0.10	0.79 ± 0.05
Thorax very slow	1.11 ± 0.10	1.21 ± 0.07	0.74 ± 0.10	0.73 ± 0.05	0.67 ± 0.10	0.76 ± 0.05	0.65 ± 0.10	0.74 ± 0.05	0.82 ± 0.10	1.04 ± 0.06
Pelvis	3.22 ± 0.11	3.48 ± 0.13	2.18 ± 0.10	2.19 ± 0.10	2.28 ± 0.10	2.06 ± 0.09	2.27 ± 0.10	1.95± 0.09	2.37 ± 0.10	2.45 ± 0.10
Spot light	5.55 ± 0.14	5.48 ± 0.19	4.21 ± 0.12	3.89 ± 0.15	3.27 ± 0.11	2.74 ± 0.11	3.69 ± 0.12	3.08 ± 0.12	4.04 ± 0.12	3.68 ± 0.14

TABLE VIII. Average dose (cGy) as measured by XRQA2 film and nanoDot OSLDs and weighted cone beam CT dose index (cGy) for all OBI CBCT imaging protocols.

Imaging protocol	nanoDot	XRQA2	CTDIw[a]
Head and neck	0.59 ± 0.04	0.45 ± 0.01	0.51
Thorax	0.56 ± 0.04	0.59 ± 0.01	0.35
Thorax very slow	0.78 ± 0.03	0.79 ± 0.02	0.44
Pelvis	2.28 ± 0.03	2.2 ± 0.03	1.39
Spot light	3.59 ± 0.04	3.32 ± 0.04	1.78

[a]$CTDI_W$ is provided by the Vendor and displayed in the system software.

When surface and internal doses for each imaging protocol are compared (Tables III and IV for the XVI system and Tables VI and VII for the OBI system), the following patterns can be observed: the surface and internal doses for the XVI head and neck protocol and also for the XVI fast head and neck protocols were within uncertainties; dose acquired during the XVI chest M20 protocol (360°) indicated that the dose increased from the right surface toward the center of the phantom and then started to decrease toward the left surface; Tables III and IV also indicated that for the XVI symmetry protocol, the anterior doses were much higher than the posterior doses and the surface doses were higher than the near surface doses. Tables VI and VII indicated that the anterior doses were higher than the posterior doses for all OBI imaging protocols investigated in this study, with the exception of the pelvis imaging protocol. They also showed that the lateral doses for each of the OBI imaging protocol are close to each other (within uncertainties) with the exception of the thorax very slow protocols, where a somewhat higher right lateral than left lateral dose was observed. The lateral internal doses were higher than the lateral surface doses for all OBI imaging protocols. The vertical internal doses were also higher than the vertical surface doses for all OBI protocols, with the exception of the thorax very slow protocol where comparable vertical surface and internal doses were observed. The variations between the surface and internal doses depend on dose profiles. We did not measure dose profiles for imaging protocols of both CBCT systems. Tomic *et al.*[3] measured dose profiles for head (200°), thorax (360°), pelvis (360°), and spotlight (200°) OBI CBCT imaging protocol (version 1.4) using Gafchromic XRQA film. They investigated thorax and pelvis protocols similar to the thorax and pelvis protocols investigated in our study (version 1.5) in terms of trajectory and our results on the surface and internal doses for the thorax and pelvis imaging protocols showed more or less similar trend to their reported dose profiles.

Tables III and IV for the XVI CBCT system and Tables VI and VII for the OBI CBCT systems indicated that both Gafchromic XRQA2 film and nanoDot OSLDs gave close estimation of the dose in many cases (within their uncertainties) and almost identical estimation of dose in some cases. However, there were some disagreements between the results obtained using the two dosimeters in which discrepancies ranged between 15% and 30%. These disagreements were particularly observed for the surface and internal doses of the XVI chest M20 protocol, the surface dose for the XVI pelvis M20 protocol, the OBI spotlight imaging protocol, and some points for the OBI thorax and pelvis imaging protocols. The observed disagreements in the measured dose between the two types of the dosimeters could be tracked back to several factors. The measured surface doses for all XVI imaging protocols were acquired during two different times (film and OSLD measurements were not taken at the same time) and this might lead to slight variations in the experiment setup. The measured internal doses using the two dosimeters for all XVI and OBI imaging protocols were acquired at the same time and the two dosimeters were placed next to each others as shown in the experimental setup schematic diagram (Fig. 1). The discrepancies between the two dosimeters at some points could be in part related to dose profiles. We did not measure any dose profiles; however, these profiles, as reported by Tomic *et al.*[3] for some OBI 1.4 imaging protocol, can vary from one protocol to another and showed that doses are not always uniform and even for those near uniform profiles, some variations in dose can happen especially near the phantom surfaces. Hence, the two dosimeters can be exposed to slightly different dose even though they are placed next to each other. The dose profiles reported by Tomic *et al.*[3] for the OBI thorax and pelvis imaging protocols support to some extent our justifications for the observed discrepancies between the two types of dosimeters at some points.

Table V showed that the average doses for each of the XVI imaging protocol obtained using both XRQA2 film and nanoDot OSLDs were similar (within uncertainties). The exception was the symmetry imaging protocol; in this case, the OSLD results were 22% higher than the XRQA result. This variation could be attributed to noticeable different doses obtained by the two dosimeters at some points (surface anterior, surface left lateral, near anterior surface, and central) and to the different relative uncertainty of the two dosimeters for XVI dose measurements (∼2% for OSLD and 4%–6% for XRQA2 film, which resulted in higher weights being assigned to high doses measured by OSLD as compared with high doses measured by the film). The results shown in Table V combined with the results given in Tables III and IV indicated that the symmetry protocol, which is a 4D protocol (A 4D-CBCT scans with the symmetry protocol take 3 min with a 200° gantry rotation. Symmetry automatically sorts images into ten phases based on automatic detection of diaphragm position.[31]) do not necessarily result in higher dose compared with other protocols, which are 3D protocols. Table V also indicated that for the XVI imaging protocols, the measured doses were in good agreement with the nominal doses provided by the Vendor. The nominal doses represent the weighted cone beam CT dose index measured in especially designed cylindrical phantoms that takes into account the wide CBCT beams.[32] Here, it should be noted that the Vendor's nominal dose is a different quantity from our measured point doses, despite the fact that they were in good agreement with our results. Table VIII showed that both XRQA2 film and nanoDot OSLDs resulted almost in the same estimation of average doses acquired during thorax, thorax very slow, and pelvis OBI imaging protocols. The

discrepancy between the results of the two dosimetry systems was 7.5% for the spot light imaging protocols and even much higher for the head and neck imaging protocol where a discrepancy of ~24% was observed. When our estimation of the average dose acquired during different OBI imaging protocols are compared with the $CBDI_w$ (provided by Vendor), one can observe a difference between the two quantities. The $CBDI_w$ for all OBI imaging protocols investigated in this study was less than our measured average doses, such a difference is expected as the two quantities are completely different. The $CBDI_w$ is usually measured in standard cylindrical acrylic phantoms (one for the head, with a diameter of 16 cm and the other for the body with a diameter of 32 cm), while our reported average doses are averages of point doses measured in anthropomorphic phantom.

It should be noted that the dose measurements in the phantom do not represent the real patient dose, as the effective atomic number and mass density of tissue and organ vary between the phantom and the human.[13] Another point deserves attention here is the fact that all our measurements were performed using the male Alderson Rando Phantom. Doses, however, vary substantially as the size of the patient/phantom change. Islam *et al.*[5] reported different patient doses for patients with different AP and lateral separation. Wen *et al.*[33] reported that the larger the patient size, the less the AP skin dose, but lateral doses do not change significantly with patient size. Abolaban[34] investigated the effect of phantom size on the measured dose and reported that CBCT dose decreased as the phantom size increased in both standard dose OBI 1.4 head and pelvis scan modes.

Previous studies performed on various versions of the XVI CBCT system reported different dose quantities including $CBDI_w$; surface dose; organ dose; and patient dose. The results of these studies follow. Amer *et al.*[6] performed measurements on Elekta synergy CBCT system (release 3.1) and reported $CBDI_w$ of 0.16 cGy for head (100 kVp and 38 mAs), 0.6 cGy for lung (120 kVp and 152 mAs), and 2.5 cGy for pelvis (130 kVp and 456 mAs) protocols. They also reported patient surface doses as high as 0.3 cGy for head and neck, 1.5 cGy for lung, and 3.4 cGy for prostate. Islam *et al.*[5] reported doses ranging from 1.2 to 2.0 cGy in 16 cm-diameter head phantom and doses ranging from 1.6 cGy (at the center) to 2.3 cGy (at the surface) in 30 cm-diameter body phantom. The settings of their imaging protocols included full rotation scans; total mAs of 660; and beam energy of 100, 120, and 140 kVp. They also reported patient skin dose ranging from 1.12 to 1.84 cGy. Song *et al.*[7] reported $CBCTDI_w$ of 0.1 and 2.4 cGy for head and neck and pelvis imaging protocols, respectively. Hyer and Hintenlang[8] calculated organ doses using ImPact patient dose calculator for XVI (Version 4.0) head, chest, and pelvis imaging protocols, the organ doses ranged from: 0.005 to 0.08 cGy in the head region from head scan; 1.5 to 2.8 cGy in the chest region from chest scan; and 1.95 to 2.2 cGy in the pelvis region from pelvis scan. Hyer *et al.*[9] reported kV XVI (software version 4.0) organ doses ranging from: 0.069 to 0.107 cGy in the head region from head scan; 1.4 to 1.7 cGy in the chest region from chest scan; and 1.6 to 2.9 cGy in the pelvis region from pelvis scan. Spezi *et al.*[10] used Monte Carlo (MC) method to calculate kV XVI CBCT mean organ dose per CBCT scan. The mean doses were: 2.4 cGy for PTV and 2.1 cGy for body in the pelvis region; 2.9 cGy for PTV and 2.0 cGy for body in the chest region; and 0.3 cGy for PTV and 0.21 cGy for body in the head and neck region. Alaei and Spezi[11] used TLDs to measure kV XVI doses in Rando Phantom and calculated dose using Pinnacle treatment planning system and Monte Carlo method. They reported average doses of the order of 0.11 cGy for head and neck, 3.3 cGy for the chest, and 2.33 cGy for the pelvis. Doses reported by Amer *et al.*[6] resulted in 25% higher CBDI than the Vendor's nominal dose (Table V); 66% higher surface dose than the average dose of the protocols investigated in our study; 12% higher CBDI than the nominal dose; and ~33% higher surface dose than the average dose of the pelvis protocol used in our study. The reported dose by Islam *et al.*[5] for the head phantom were 12–20 times higher than our average doses for the head and neck, however, our reported doses in other body regions were within their reported values for the body phantom, despite some differences in the protocol settings. Doses reported by Song *et al.*[7] on average dose index for the head and neck protocol was very close to the average dose and the nominal dose of our study. However, their estimation of the $CBCTDI_w$ for the pelvis protocol was 8% higher than the average dose and the nominal dose listed in Table V. Our estimation of average doses (Table V) were within the range of organ doses for head, chest, and pelvis imaging protocols (XVI version 4.0) reported by Hyer and Hintenlang[8] and Hyer *et al.*[9] Our results (Table V) were comparable to those reported by Spezi *et al.*[10] for the pelvis and chest regions and much lower than those for head and neck protocols. Alaei and Spezi[11] reported similar pelvis and head and neck doses to ours and about 20% higher than our result for the chest region.

Previous studies were also performed on various versions of the OBI CBCT system. Ding *et al.*[4] reported that doses to soft tissues, such as eye, spinal cord, and brain, from a typical head and neck scan can be as high as 8, 6, and 5 cGy, respectively, and doses to bone can be as high as 25 cGy. Song *et al.*[7] reported $CBCTDI_w$ of 8.3 and 5.4 cGy for head and body phantoms, respectively. Palm *et al.*[12] measured dose in transverse planes of the Alderson phantom for different OBI (ver. 1.3 and ver. 1.4) imaging protocols. For OBI ver. 1.3, doses were between 6.4 and 14.4 cGy, with average dose of around 10 cGy. For OBI ver. 1.4, measured doses were between 0.1 and 5.1 cGy, with mean dose range between 0.3 and 3.5 cGy. Tomic *et al.*[3] reported OBI CBCT (ver. 1.4) surface doses ranging from: 0.1 to 3.69 cGy using different head and neck protocols; 0.99 to 1.34 cGy using low dose thorax protocol; and 0.46 to 4.7 cGy using a pelvis imaging protocol. Kim *et al.*[16] reported $CTDI_w$ for different OBI (version 1.4) imaging protocols ranging from: 0.32 to 2.9 cGy (compared to 8.4 cGy from older standard head protocol) for different head scans; 2.4 to 2.5 cGy (compared to 4.6 cGy from older standard body protocol) for pelvis scans; and 0.77 cGy for low dose thorax scan. Hyer and Hintenlang[8] reported organ doses calculated using ImPact patient dose calculator ranging from: 0.008 to 0.0.38 cGy in the head region from head scan;

0.51 to 1.1 cGy in the chest region from chest scan; and 2.1 to 2.2 cGy in the pelvis region from pelvis scan. Hyer *et al.*[9] measured kV OBI (software version 1.4.13) organ doses acquired during the same protocols they used in their other study,[8] doses ranged from: 0.11 to 0.30 cGy in the head region from head scan; 0.43 to 0.53 cGy within the chest region from chest scan; and 1.5 to 3.5 cGy in the pelvis region from pelvis scan. Cheng *et al.*[13] measured organ doses for kV OBI (software versions 1.4.13 and 1.4.11) ranging from: 0.002 to 1.8 cGy (OBI version 1.4.13); 0.008 to 9.4 cGy (OBI version 1.4.11) in different body organs from head scan; 0.004 to 3.04 cGy (OBI version 1.4.13)' and 0.008 to 5.9 cGy (OBI version 1.4.11) in different body organs from pelvis scan. Our results of the surface dose were comparable to those reported by Tomic *et al.*[3] on OBI 1.4 system for the head and neck scan and much lower for the thorax and pelvis scans. The average doses (which are average doses in the irradiated area and not specific organ doses) of the scans investigated in this study (Table VIII) were well with the ranges of organ doses reported by Cheng *et al.*[13] and higher than organ doses reported by Hyer *et al.*[9] for head and chest scans and within the range of doses reported for the pelvis scans. Our measured average doses were comparable to the mean doses reported by Palm *et al.*[12] The values of the $CTDI_W$ provided by the Vendor (Table VIII) of OBI True beam 1.5 are well below those measured by Song *et al.*[7] and Kim *et al.*[16] for older OBI imaging protocols.

Regardless the fact that different methods (measurements or MC calculations) and dosimeters were used to measure CBCT dose during different versions of XVI and OBI CBCT systems and different dose levels were reported, it is clear that new versions of the CBCT systems imaging protocols resulted in lower doses compared with earlier versions. A complete comparison between doses imparted during different imaging protocols using different CBCT systems should give consideration to other factors such as image quality. To the best of our knowledge, this paper is the first paper to report on the effects of different CBCT beam qualities on the dose response curves of Gafchromic XRQA2 film and nanoDot OSLD and also on doses acquired during Elekta XVI (version R4.5) and Varian OBI (version 1.5) CBCT scans.

V. CONCLUSIONS

Dose response curves for Gafchromic XRQA2 film and nanoDot OSLDs should be generated for all irradiation settings to ensure accurate estimation of measured dose. Differences in the response curves of both Gafchromic XRQA2 film and nanoDot OSLD were observed even at the same photon energy when different filters were used. The percentage total relative uncertainties for both Gafchromic and nanoDot OSLDs were below 6% at doses above 1 cGy. Both dosimetry systems gave close estimation of CBCT doses in most cases, with the exception of some noticeable differences at some measured point doses. Gafchromic XRQA2 film and nanoDot OSLD resulted in almost equal values (within uncertainty level) for average dose acquired during the different XVI and OBI CBCT imaging protocols investigated in this study. The exceptions were the doses of the symmetry (XVI protocol) and spot light (OBI protocol) protocols. The measured average doses of the XVI imaging protocols were also comparable to the nominal dose provided by the Vendor. There were differences between the measured average doses of the OBI imaging protocols and the $CBDI_w$ provided by the Vendor. New versions of the CBCT systems imaging protocols resulted in lower doses compared with earlier versions.

ACKNOWLEDGEMENT

This project is funded, in part, under a grant with the Pennsylvania Department of Health. The Department specifically declaims responsibility for any analyses, interpretations or conclusions.

[a]Author to whom correspondence should be addressed. Electronic mail: ying.xiao@jeffersonhospital.org

[1]C. Walter, J. Boda-Heggemann, H. Wertz, I. Loeb, A. R. F. Lohr, and F. Wenz, "Phantom and *in*-vivo measurements of dose exposure by image-guided radiotherapy (IGRT): MV portal images vs. kV portal images vs. cone-beam CT," Radiother. Oncol. **85**, 418–423 (2007).
[2]M. F. Chan, J. Yang, Y. Song, C. Burman, P. Chan, and S. Li, "Evaluation of imaging performance of major image guidance systems," Biomed. Imaging Interv. J. **7**(2) (2011).
[3]N. Tomic, S. Devic, F. DeBlois, and J. Seuntjens, "Reference Radiochromic film dosimetry in kilovoltage photon beams during CBCT image acquisition," Med. Phys. **37**(3), 1083–1092 (2010).
[4]G. X. Ding, D. M. Duggan, and C. W. Coffey, "Accurate patient dosimetry of kilovoltage cone-beam CT in radiation therapy," Med. Phys. **35**(3), 1135–1144 (2008).
[5]M. K. Islam, T. G. Purdie, B. D. Norrlinger, H. Alasti, D. J. Moseley, M. B. Sharpe, J. H. Siewerdsen, and D. A. Jaffray, "Patient dose from kilovoltage cone beam computed tomography imaging in radiation therapy," Med. Phys. **33**(6), 1573–1582 (2006).
[6]A. Amer, T. Marchant, J. Sykes, J. Czajka, and C. Moore, "Imaging doses from the Elekta Synergy X-ray cone beam CT system," Br. J. Radiol. **80**, 476–482 (2007).
[7]W. Y. Song, S. Kamath, S. Ozawa, S. Al Ani, A. Chvetsov, N. Bhandare, J. R. Palta, C. Liu, and J. G. Li, "A dose comparison study between XVI® and OBI® CBCT systems," Med. Phys. **35**(2), 480–486 (2008).
[8]D. E. Hyer and D. E. Hintenlang, "Estimation of organ doses from kilovoltage cone-beam CT imaging used during radiotherapy patient position verification," Med. Phys. **37**(9), 4620–4626 (2010).
[9]D. E. Hyer, C. F. Serago, S. Kim, J. G. Li, and D. E. Hintenlang, "An organ and effective dose study of XVI and OBI cone-beam CT systems," J. Appl. Clin. Med. Phys. **11**(2), 181–197 (2010).
[10]E. Spezi, P. Downes, R. Jarvis, E. Radu, and J. Staffurth, "Patient-specific three dimensional concomitant dose from computed tomography exposure in image guided radiotherapy," Int. J. Radiat. Oncol., Biol., Phys. **83**(1), 419–426 (2012).
[11]P. Alaei and E. Spezi, "Commissioning kilovoltage cone-beam CT beams in a radiation therapy treatment planning system," J. Appl. Clin. Med. Phys. **13**(6), 19–33 (2012).
[12]A. Palm, E. Nilsson, and L. Hernsdorf, "Absorbed dose and dose rate using the Varian OBI 1.3 and 1.4 CBCT system," J. Appl. Clin. Med. Phys. **11**(1), 229–240 (2010).
[13]H. C. Y. Cheng, V. W. C. Wu, E. S. F. Liu, and D. L. W. Kwong, "Evaluation of radiation dose and image quality for the Varian cone beam computed tomography system," Int. J. Radiat. Oncol., Biol., Phys. **80**(1), 291–300 (2011).
[14]G. X. Ding and C. W. Coffey, "Beam characteristics and radiation output of a kilovoltage cone-beam CT," Phys. Med. Biol. **55**, 5231–5248 (2010).
[15]E. Spezi, P. Downes, E. Radu, and R. Jarvis, "Monte Carlo simulation of an x-ray volume imaging cone beam CT unit," Med. Phys. **36**(1), 127–136 (2009).
[16]S. Kim, S. Yoo, F.-F. Yin, E. Samei, and T. Yoshizumi, "Kilovoltage cone-beam CT: Comparative dose and image quality evaluations in partial and full-angle scan protocols," Med. Phys. **37**(7), 3648–3659 (2010).

[17]E. K. Osei, B. Schaly, A. Fleck, P. Charland, and R. Barnett, "Dose assessment from an online kilovoltage imaging system in radiation therapy," J. Radiol. Prot. **29**, 37–50 (2009).
[18]N. Wen, H. Guan, R. Hammoud, D. Pradhan, T. Nurushev, Q. Chen, S. Li, and B. Movsas, "Dose delivered from daily CBCT to patients receiving RT for H/N and prostate cancer," Int. J. Radiat. Oncol., Biol. Phys. **66**(3), S624 (2006).
[19]T. Giaddui, Y. Cui, J. Galvin, Y. Yu, and Y. Xiao, "Surface dose measurements of kV XVI cone-beam CT system using NanoDot optical stimulated luminescence dosimeters," IFMBE Proc. **39**, 1195–1198 (2013).
[20]T. Giaddui, Y. Cui, J. Galvin, W. Chen, Y. Yu, and Y. Xiao, "Characteristics of Gafchromic XRQA2 films for kV image dose measurement," Med. Phys. **39**(2), 842–850 (2012).
[21]Landauer, Inc. 2012 Product Specifications (available URL: http://pdf.directindustry.com/pdf/landauer/microstar-dosimetry-system-specifications-and-information/23670-77698.html).
[22]C. S. Reft, "The energy dependence and dose response of commercial optical stimulated luminescent detector for kilovoltage photon, mega-voltage photon, and electron, proton and carbon beam," Med. Phys. **36**, 1690–1698 (2009).
[23]P. A. Jursinic, "Characterization of optically stimulated luminescent dosimeters, OSLDs, for clinical dosimetric measurements," Med. Phys. **34**(12), 4594–4604 (2007).
[24]C. J. Yahnke, "Calibrating the microStar," InLight TM Landuaer, Inc. 2010 (internal Report).
[25]International Speciality Product (ISP), "Gafchromic XR-QA2 film for radiology applications: Product specification sheet," see http://online1.ispcorp.com/en-US/gafchromic/SupportingDocuments/GAFCHROMIC/XRSeries.pdf.
[26]S. Brady, T. Yoshizumi, G. Toncheva, and D. Frush, "Implementation of radiochromic film dosimetry protocol for volumetric dose assessments to various organs during diagnostic CT procedures," Med. Phys. **37**(9), 4782–4792 (2010).
[27]H. Alnawaf, T. Cheung, M. J. Buston, and P. K. N. Yu, "Scanning orientation and polarization effect for XRQA radiochromic film," Radiat. Meas. **45**, 129–132 (2010).
[28]I. Mrcela, T. Bokulic, J. Izewska, M. Budanec, A. Frobe, and Z. Kusix, "Optically stimulated luminescence *in vivo* dosimetry for radiotherapy: Physical characterization and clinical measurements in 60Co beams," Phys. Med. Biol. **56**, 6065–6082 (2011).
[29]L. Lavoie, M. Ghita, L. Brateman, and M. Arreola, "Characterization of a commercially available optical stimulated luminescent dosimetry system for use in computed tomography," Health Phys. **101**, 299–310 (2011).
[30]C.-M Ma, C. W. Coffey, L. A. DeWerd, C. Liu, R. Nath, S. M. Seltzer, and J. P. Seuntjens, "AAPM protocol for 40- 300 kV x-ray beam dosimetry in radiotherapy and radiobiology," Med. Phys. **28**(6), 868–893 (2001).
[31]C. Peng, K. Chapman, B. Lu, M. Werner-Wasik, and Y. Yu, "SU-E-J-12: Initial clinical experiences in using 4D-CBCT as image guidance for lung SBRT," Med. Phys. **39**, 3654 (2012).
[32]kV XVI CBCT (Version R 4.5) Elekta Synergy (Elekta, Crawley, UK) Manual.
[33]N. Wen, H. Guan, R. Hammoud, D. Pradhan, T. Nurushev, S. Li, and B. Movsas, "Dose delivered from Varian's CBCT to patients receiving IMRT for prostate cancer," Phys. Med. Biol. **52**, 2267–2276 (2007).
[34]F. A. Abolaban, "On board cone beam CT for treatment planning in image guided radiotherapy," Ph.D. thesis, The University of Surrey, United Kingdom, 2011.